molecules

MDPI

Article

HPLC-ESI-MS^n Identification and NMR Characterization of Glucosyloxybenzyl 2*R*-Benzylmalate Deriva-Tives from *Arundina Graminifolia* and Their Anti-Liver Fibrotic Effects In Vitro

Qingqing Liu, Feiyi Sun, Yulin Deng, Rongji Dai and Fang Lv *

Beijing Key Labrotary for Separation and Analysis in Biomedicine and Pharmaceuticals, School of Life Science, Beijing Institute of Technology, Beijing 100081, China; lqq765946474@163.com (Q.L.); sfyjet@163.com (F.S.); deng@bit.edu.cn (Y.D.); dairongji@bit.edu.cn (R.D.)

* Correspondence: lvfangbeijing@bit.edu.cn; Tel.: +86-010-68949331

Received: 1 January 2019; Accepted: 29 January 2019; Published: 31 January 2019

Abstract: Four new glucosyloxybenzyl 2*R*-benzylmalate derivatives, named Arundinoside H (**2**), I (**5**), J (**6**), K (**8**) as well as four known compounds Arundinoside D (**1**), G (**3**), F (**4**), E (**7**) were isolated and characterized by a combination of chemical and spectroscopic methods, including HR-ESI-MS, 1D and 2D NMR experiments. Besides, 24 unreported compounds were inferred from ESI-MS^n data. The anti-liver fibrotic activities of the isolates were determined as proliferation inhibition of lipopolysaccharide (LPS)-induced activation of rat hepatic stellate cells (HSC-T6). The result suggested Arundinosides D, H, F, I and K showed moderate inhibitory effects in vitro.

Keywords: *Arundina graminifolia*; glucosyloxybenzyl 2*R*-benzylmalates; MS^n fragmentation pattern; anti-liver fibrotic effects

1. Introduction

Arundina graminifolia (D. Don) Hochr., a species widely distributed in subtropical Asia and known as bai-yang-jie in Chinese, has a long history of use as one of the major drugs in a formula "BaoGan Capusle" with the efficacy of heat clearing and detoxifying, dispersing blood and relieving pain, reducing inflammation and promoting urination and so on [1]. Previous phytochemical investigation focusing on the chloroform and ethyl acetate exacts of *A. graminifolia* had resulted in the separation of stilbenoids [2–4], phenols [5–7], flavonoids [8,9] and other ketones [3,10,11]. However, the works on the polar parts of the plant are few.

In the course of our studies on pharmacology, it was proved that the formula "BaoGan Capusle" was effective in the treatment of hepatic fibrosis and liver injury of model rat [12–15]. As a continuing study on bioactive constituents of *A. graminifolia*, a series of phytochemical and biological experiments of the *n*-butanol (*n*-BuOH) extract was thus performed to yield the isolation of four new and four known glucosyloxybenzyl 2*R*-benzylmalates. In this paper, we described the isolation and structural elucidation of these derivatives, as well as their anti-liver fibrotic activities in vitro. Furthermore, the fragmentation pathways of eight isolates were studied in positive ESI-MS^n, and then 24 unreported glucosyloxybenzyl 2*R*-benzylmalate derivatives were predicted by HPLC-ESI-MS^n.

2. Results and Discussion

Through the combination of various chromatographic analyses, the *n*-BuOH extraction of *A. graminifolia* was separated carefully. Four new glucosyloxybenzyl 2*R*-benzylmalates Arundinoside H

(**2**), I (**5**), J (**6**), K (**8**), as well as four known compounds Arundinoside D (**1**), G (**3**), F (**4**), E (**7**) [16] were obtained and determined by 1D and 2D NMR, and HR-ESI-MS spectra (see Supplementary Material). All these compounds were obtained as white amorphous powder. The ^{1}H and ^{13}C NMR data of the isolates were listed in Tables 1 and 2, and their structures were shown in Figure 1. The target glucosyloxybenzyl 2*R*-benzylmalates in Table 4 were observed in the positive ion mode spectra (see Supplementary Material).

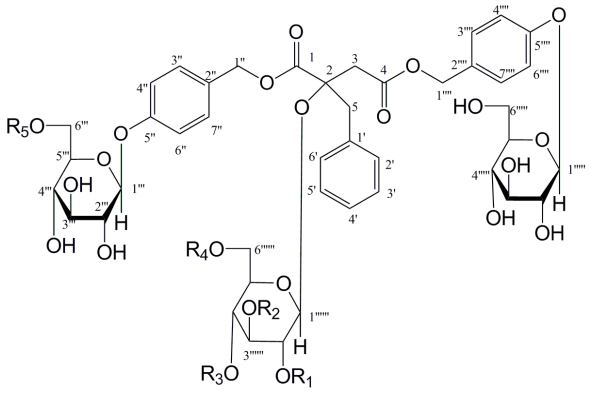

Compounds	R1 (2‴‴‴‴‴)	R2 (3‴‴‴‴‴)	R3 (4‴‴‴‴‴)	R4 (6‴‴‴‴‴)	R5 (6‴)
1	Ac	Ac	Ac	Ac	H
2	H	H	H	H	H
3	Ac	H	H	H	H
4	Ac	H	H	Ac	H
5	Ac	H	Ac	Ac	H
6	Ac	H	H	Ac	Ac
7	Ac	Ac	H	Ac	H
8	Ac	Ac	H	Ac	Ac

Figure 1. Structures of compounds **1**~**8.**

Table 1. ^{1}H nuclear magnetic resonance (NMR) data of four new compounds (700 MHz, DMSO-d6).

Position	2	5	6	8
3	2.96 (d, 17.7); 2.82 (d, 17.7)	2.96 (d, 15); 2.90 (d, 15)	2.96 (d, 17.8); 2.90 (d, 17.8)	2.96 (d, 17.8); 2.92 (d, 17.8)
5	3.17 (m); 3.06 (m)	3.10 (d, 14); 3.02 (d, 14)	3.10(d, 14); 3.02 (d, 14)	3.10 (d, 14); 3.02 (d, 14)
2′, 6′	7.19 (m)	7.18 (m)	7.18 (m)	7.18 (m)
3′, 5′	7.16 (m)	7.02 (m)	7.01 (d, 8.7)	7.01 (d, 8.7)
4′	7.19 (m)	7.18 (m)	7.17 (m)	7.17 (m)
1″	4.99 (d, 7.9); 4.90 (d, 7.9)	5.00 (d, 12); 4.92 (d, 12)	5.00 (d, 12); 4.93 (d,12)	5.00(d,12); 4.93 (d,12)
3″, 7″	7.27 (d, 8.4)	7.27 (d, 8.3)	7.27 (d, 8.7)	7.27 (d, 8.7)
4″, 6″	7.01 (d, 8.5)	7.02 (m)	7.01 (d, 8.7)	7.01 (d, 8.7)
Glc-1‴	4.87 (d, 7.5)	4.91 (d, 7.9)	4.92 (d, 7.5)	4.92 (d, 7.7)
Glc-2‴	3.27 (m)	3.26 (m)	3.27 (m)	3.27 (m)
Glc-3‴	3.24 (m)	3.23 (m)	3.22 (m)	3.22 (m)
Glc-4‴	3.16 (m)	3.16 (m)	3.18 (m)	3.18 (m)
Glc-5‴	3.27 (m)	3.26 (m)	3.27 (m)	3.27 (m)
Glc-6‴	3.68 (m); 3.47 (m)	3.68 (m); 3.46 (m)	4.27 (m); 4.08 (m)	4.27 (m); 4.08 (m)
Glc-6‴-$COCH_3$	-	-	1.99 (s)	1.99 (s)
1⁗	5.01 (d, 12); 4.90 (d, 12)	5.04 (d, 12); 4.91 (d, 12)	5.00 (d, 12); 4.99 (d, 12)	5.00 (d,12); 4.99 (d,12)
3⁗, 7⁗	7.25 (d, 8.4)	7.23 (d, 8.3)	7.23 (d, 8.7)	7.23 (d, 8.7)
4⁗, 6⁗	7.02 (d, 8.5)	7.02 (m)	7.02 (d, 8.7)	7.02 (d, 8.7)
Glc-1⁗	4.87 (d, 7.5)	4.86 (d, 7.7)	4.92 (d, 7.5)	4.87 (d, 7.5)
Glc-2⁗	3.27 (m)	3.16 (m)	3.30 (m)	3.30 (m)
Glc-3⁗	3.24 (m)	3.23 (m)	3.22 (m)	3.22 (m)
Glc-4⁗	3.16 (m)	3.16 (m)	3.18 (m)	3.18 (m)
Glc-5⁗	3.27 (m)	3.26 (m)	3.27 (m)	3.27 (m)
Glc-6⁗	3.69 (m); 3.47 (m)	3.68 (m); 3.46 (m)	3.68 (m); 3.46 (m)	3.68 (m); 3.46 (m)
Glc-1′′′′′′	4.66 (d, 7.8)	4.94 (d, 8.0)	4.86 (d, 7.6)	5.05 (d, 8.0)
Glc-2′′′′′′	3.03 (m)	4.68 (m)	4.56 (m)	4.69 (m)
Glc-3′′′′′′	3.39 (m)	3.46 (m)	3.68 (m)	4.93 (m)
Glc-4′′′′′′	4.36 (m)	4.64 (m)	3.46 (m)	3.46 (m)
Glc-5′′′′′′	3.52 (m)	3.45 (m)	3.61 (m)	3.61 (m)
Glc-6′′′′′′	3.68 (m); 3.38 (m)	4.05 (m); 3.76 (m)	4.08 (m); 4.05 (m)	4.08 (m); 4.05 (m)
Glc-2′′′′′′-$COCH_3$	-	1.70 (s)	1.72 (s)	1.65 (s)
Glc-3′′′′′′-$COCH_3$	-	-	-	1.92 (s)
Glc-4′′′′′′-$COCH_3$	-	2.01 (s)	-	
Glc-6′′′′′′-$COCH_3$	-	1.92 (s)	1.92 (s)	1.99 (s)

Table 2. ^{13}C NMR data of four new compounds (175MHz, DMSO-d6).

Position	2	5	6	8
1	170.9	170.1	170.5	170.1
2	79.8	80.7	81.0	81.3
3	40.4	40.9	41.0	41.0
4	169.8	169.5	170.1	170.1
5	42.0	43.6	43.8	43.7
1′	135.5	135.0	135.5	135.4
2′, 6′	127.9	127.9	128.3	128.3
3′, 5′	130.6	130.5	130.9	130.9
4′	126.7	126.7	127.1	127.1
1″	66.3	66.2	66.6	66.6
2″	128.9	128.8	129.3	129.2
3″, 7″	129.9	129.9	130.3	130.3
4″, 6″	116.2	116.2	116.7	116.7
5″	157.4	157.4	157.9	157.9
Glc-1‴	100.3	100.3	100.5	100.5
Glc-2‴	76.8	76.6	77.1	77.1
Glc-3‴	73.2	73.2	73.5	73.6
Glc-4‴	69.6	69.7	70.1	70.2
Glc-5‴	76.6	76.6	76.8	76.8
Glc-6‴	60.7	60.7	63.9	63.8
Glc-6‴-$COCH_3$	-	-	170.7; 21.2	170.7; 21.1
1⁗	65.6	65.7	66.2	66.2
2⁗	128.8	128.6	129.3	129.3
3⁗, 7⁗	129.9	129.9	130.4	130.4
4⁗, 6⁗	116.1	116.2	116.5	116.5
5⁗	157.4	157.4	157.6	157.6
Glc-1⁗′	100.3	100.4	100.8	100.8
Glc-2⁗′	76.8	77.0	77.5	77.5
Glc-3⁗′	73.2	73.2	73.6	73.4
Glc-4⁗′	69.6	70.3	70.1	70.1
Glc-5⁗′	76.6	76.6	76.8	76.8
Glc-6⁗′	60.7	60.7	61.1	61.1
Glc-1⁗″	98.3	96.7	97.0	96.7
Glc-2⁗″	77.0	70.9	73.8	71.2
Glc-3⁗″	73.7	70.9	74.0	75.1
Glc-4⁗″	69.7	72.8	73.7	67.9
Glc-5⁗″	76.7	70.6	74.1	74.1
Glc-6⁗″	61.2	61.8	63.3	62.9
Glc-2⁗″-$COCH_3$	-	169.7; 20.5	169.8; 21.0	169.6; 20.7
Glc-3⁗″-$COCH_3$	-	-	-	170.3; 21.0
Glc-4⁗″-$COCH_3$	-	169.3; 20.8	-	-
Glc-6⁗″-$COCH_3$	-	170; 20.7	170.7; 21.1	170.1;21.2

2.1. Structure Elucidation of New Compounds

The HR-ESI-MS showed a $[M + NH_4]^+$ ion at m/z 1066.3764, from which the molecular formula of compound **6** was determined to be $C_{49}H_{60}O_{25}$. The ^1H and ^{13}C NMR data (Tables 1 and 2) showed signals for four methylene groups at δ_C 41.0 (C-3), δ_H 2.96 (1H, d, J = 17.8 Hz, H-3), 2.90 (1H, d, J = 17.8 Hz, H-3); δ_C 43.8 (C-5), δ_H 3.10 (1H, d, J = 13.8 Hz, H-5), 3.02 (1H, d, J = 14 Hz, H-5); δ_C 66.6 (C-1″), δ_H 5.00 (1H, d, J = 12 Hz, H-1″), 4.93 (1H, d, J = 12 Hz, H-1″); δ_C 66.2 (C-1⁗), δ_H 5.00 (1H, d, J = 12 Hz, H-1⁗), 4.99 (1H, d, J = 12 Hz, H-1⁗). One quaternary carbon at δ_C 81.0 (C-2) and two carbonyl groups at δ_C 170.5 (C-1), and δ_C 170.1 (C-4) were ascertained by comparing ^{13}C NMR and DEPT spectra, which indicated the basic structure as malic acid [17]. The HMBC correlarions

from H_2-3 to C-1, C-2 and C-4; H_2-5 to C-1 and C-2, combined the comparison of 1D NMR spectra of compound 6 with those of Arundinoside D~F, indicated the presence of 2*R*-malic acid moiety.

Through the proton signals at δ_H 7.18 (2H, H-2′/6′), 7.01 (2H, H-3′/5′), 7.17 (1H, H-4′), and the ^{13}C signals at δ_C 135.5 (C-1′), 128.3 (C-2′/6′), 130.9 (C-3′/5′), 127.1 (C-4′), the benzene group was identified, combining at C-5 based on HMBC correlation between C-1′ and H_2-5. Other two benzene groups were identified by the proton signals at δ_H 7.01 (4H, H-4″/6″/H-4‴/6‴), 7.23 (2H, H-3‴/7‴), 7.27 (2H, H-3″/7″), and the carbon signals at δ_C 157.9 (C-5″), 157.6 (C-5‴), 130.3 (C-3″/7″/C-3‴/7‴), 129.3 (C-2″/2‴), 116.7 (C-4″/6″), 116.5 (C-4‴/6‴). According to HMBC correlations between H_2-1″ and C-2″, H_2-1‴ and C-2‴, the substitution positions of the benzene groups were C-1″ and C-1‴, respectively.

The ^1H NMR spectrum of compound **6** showed well-resolved signals for three anomeric protons of three glucoses at δ_H 4.92 (2H, d, *J* = 7.5 Hz, H-Glc-1⁗/1⁗′) and 4.86 (1H, d, *J* = 7.5 Hz, H-Glc-1⁗′). The splitting patterns of anomeric proton signals indicated that the sugar units were β-linkage [18]. The long-correlations from H-1⁗ to C-5″, H-1⁗′ to C-5‴, H-1⁗′ to C-2 in HMBC experiment ascertained the sugar units combined at C-5″, C-5‴ and C-2, respectively. The absolute configuration of the glucoses was D-form by the hydrolysis process [19].

In ^1H and ^{13}C NMR spectra, acetyl methyl protons at δ_H 1.72 (s), 1.92 (s), 1.99 (s) and acetyl carbonyl carbons at δ_C 169.8 (C), 170.7 (2C) indicated compound **6** possessed three acetyl groups, and the substitution positions were C-6⁗, C-2⁗′, C-6⁗′ by HMBC correlations from δ_H 4.27/4.08 (2H, m, H_2-6⁗) to 170.7, 4.56 (1H, m, H-2⁗′) to δ_C 169.8, 4.08/4.05 (2H, m, H_2-6⁗′) to 170.7. The key HMBC correlations of compound **6** were showed in Figure 2. All the protons and carbons were well assigned by NMR analysis. Therefore, compound **6** was determined as 1-(β-D-glucopyranosyloxybenzyl-6⁗-acetyl)-2-(β-D-glucopyranosyl-2⁗′,6⁗′-diacetyl)-4-(β-D-glucopyranosyloxybenzyl)-2*R*-benzylmalate, and named Arundinoside J.

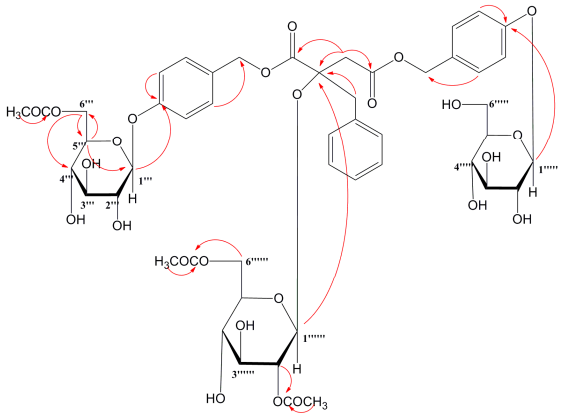

Figure 2. Key HMBC correlations of compound **6.**

The molecular formula of compound **5** was determined to be $C_{49}H_{60}O_{25}$ based on the HR-ESI-MS ion $[M + NH_4]^+$ at *m*/*z* 1066.3766. ^1H and ^{13}C NMR data of compound 5 indicated that it was a glucosyloxybenzyl 2*R*-benzylmalate derivative with three acetyl groups as the same as compound 6, but one group substituted position was different. The structure of compound **5** was further confirmed by HSQC and HMBC experiments. The substituent positions of three acetyl groups were determined at C-2⁗′, C-4⁗′ and C-6⁗′ according to HMBC correlations from δ_H 4.68 (1H, m, H-2⁗′) to δ_C 169.7, 4.64 (1H, m, H-4⁗′) to 169.3, 4.05/3.76 (2H, m, H_2-6⁗′) to 170.0. Therefore, compound **5** was identified as 1-(β-D-glucopyranosyloxybenzyl)-2-(β-D-glucopyranosyl-2⁗′,4⁗′,6⁗′-triacetyl)-4-(β-D-glucopyranosyloxybenzyl)-2*R*-benzylmalate, and named Arundinoside I.

The molecular formula of compound **8** was determined to be $C_{51}H_{62}O_{26}$ based on the HR-ESI-MS ion $[M + NH_4]^+$ at *m*/*z* 1108.3869. ^1H and ^{13}C NMR data indicated the structure of compound **8** was a

glucosyloxybenzyl 2*R*-benzylmalate derivative with four acetyl groups. Further analysis of HMBC correlations from δ_H 4.08/4.27 (2H, m, H_2-6‴) to 170.7, 4.69 (1H, m, H-2⁗) to 169.6, 4.93 (1H, m, H-3⁗) to 170.3, 4.05/4.08 (2H, m, H-6⁗) to 170.1 suggested that four acetyl groups of compound **8** substituted at C-6‴, C-2⁗, C-3⁗, C-6⁗, respectively. Therefore, compound **8** was identified as 1-(β-D-glucopyranosyloxybenzyl-6‴-acetyl)-2-(β-D-glucopyranosyl-2⁗,3⁗,6⁗-triacetyl)-4-(β-D-glucopyranosyloxybenzyl)-2*R*-benzylmalate, and named Arundinoside K.

The molecular formula of compound **2** was determined to be $C_{43}H_{54}O_{22}$ based on the HR-ESI-MS ion $[M + NH_4]^+$ at *m*/*z* 940.3453. ^1H and ^{13}C NMR data showed compound **2** was a glucosyloxybenzyl 2-benzylmalate derivative without acetyl group, and its structure was further confirmed by HSQC and HMBC experiments. Therefore, compound **2** was identified as 1-(β-D-glucopyranosyloxybenzyl)-2-(β-D-glucopyranosyl)-4-(β-D-glucopyranosyloxy-benzyl)-2*R*-benzylmalate, and named Arundinoside H.

2.2. MS Fragmentation Pattern

HPLC-ESI-MS^n experiments were carried out to analysis structural characterization and discuss the fragmentation behaviors of glucosyloxybenzyl 2*R*-benzylmalates **1**–**8** from *A. graminifolia*. The target glucosyloxybenzyl 2*R*-benzylmalates recorded at retention times were designed as A1–A6, B1–B6, C1–C3, D1–D6. The positive ion mode was performed on each of these components, and ESI-MS^n data were summarized in Tables 3 and 4.

Table 3. HR-ESI-MS and key ESI-MS^n data of the isolates **1**–**8**.

Compounds	Molecular Formula	HR-ESI-MS $[M + NH_4]^+$	ESI-MS^1: $[M + Na]^+$	ESI-MS^n
1	$C_{51}H_{62}O_{26}$	1108.3861	1113	845, 577, 515, 497, 371, 353, 311, 251, 247
2	$C_{43}H_{54}O_{22}$	940.3453	945	677, 515, 409, 247
3	$C_{45}H_{56}O_{23}$	982.3554	987	719, 515, 451, 247
4	$C_{47}H_{58}O_{24}$	1024.3665	1029	761, 515, 493, 287, 269, 247, 227
5	$C_{49}H_{60}O_{25}$	1066.3766	1071	803, 535, 329, 311, 269, 247
6	$C_{49}H_{60}O_{25}$	1066.3764	1071	761, 515,493, 287, 269, 247
7	$C_{49}H_{60}O_{25}$	1066.3766	1071	803, 535, 515, 329, 311, 247, 209
8	$C_{51}H_{62}O_{26}$	1108.3869	1113	803, 535, 515, 329, 311, 247, 209

Table 4. Key ESI-MS^n Fragment Ions and structural information of the components predicted.

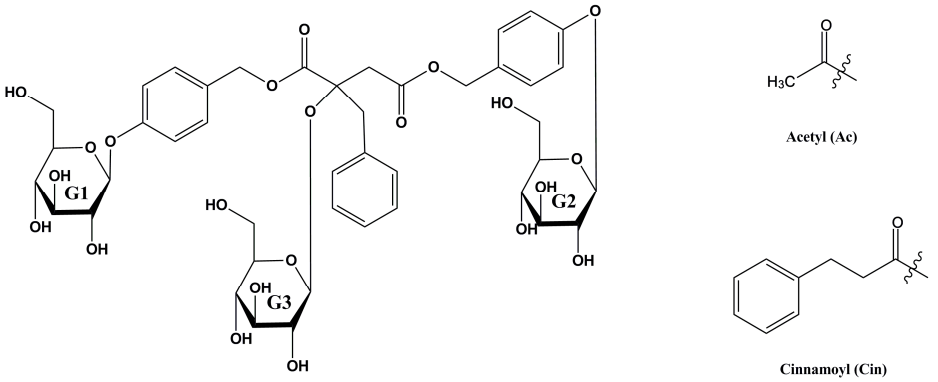

Peaks	RT	MS^1 $[M + Na]^+$	MS^n	G1	G2	G3
A1	3.9 min	1006	1029, 761, 515, 493, 287, 269, 247			2Ac
A2	6.4 min	1048	1071, 803, 535, 515, 329, 311			3Ac
A3	7.3 min	1048	1072, 761, 515, 493, 287, 269, 247	Ac		2Ac
A4	12.7 min	1090	1113, 845, 535, 329, 311		Ac	3Ac
A5	13.9 min	1090	1113, 803, 535, 329, 311, 247	Ac		3Ac
A6	14.0 min	1052	1071, 677, 515, 247	Cin		
A7	22.2 min	1094	1117, 849, 645, 247		Cin	Ac
A8	21.1 min	1090	1113, 845, 535, 329, 247		Ac	3Ac
A9	28.0 min	1094	1117, 719, 451, 247	Cin		Ac

Table 4. *Cont.*

Peaks	RT	MS^1 $[M + Na]^+$	MS^n	G1	G2	G3
B1	3.7 min	964	987, 719, 515, 247			Ac
B2	4.3 min	964	987, 719, 515, 247			Ac
B3	7.0 min	760	783, 515, 247			OH
B4	9.0 min	1006	1029, 761, 557, 451, 247		Ac	Ac
B5	11.0 min	1006	1029, 719, 515, 451, 247	Ac		Ac
B6	12.6 min	1006	1029, 761, 515, 493, 287, 269, 247			2Ac
C1	6.4 min	1048	1071, 761, 557, 451, 247	Ac	Ac	Ac
C2	8.9 min	1048	1071, 761, 515, 493, 287, 269, 247	Ac		2Ac
C3	11.9 min	1048	1071, 803, 535, 329, 311, 269, 247			3Ac
D1	16.0 min	1252	1275, 845, 577, 371, 353, 311			4Ac
D2	8.5 min	1052	1075, 677, 515, 247	Cin		
D3	7.0 min	1052	1075, 677, 515, 247	Cin		
D4	15.6 min	1094	1117, 719, 515, 451, 247	Cin		Ac
D5	18.6 min	1094	1117, 719, 515, 451, 247	Cin		Ac
D6	19.3 min	1094	1117, 719, 515, 451, 247	Cin		Ac

2.2.1. MS Fragmentation Pathway of Glucosyloxybenzyl 2*R*-Benzylmalate Derivatives Isolated

In ESI-MS^1 spectrum of compound **6** (Figure 3a), significant molecular ion peaks at m/z 1066 $[M + NH_4]^+$, 1071 $[M + Na]^+$,1087 $[M + K]^+$ were observed, among which the $[M + Na]^+$ and product ions were sufficient abundance for further analysis. In ESI-MS^2 spectrum of compound **6** (Figure 3b), the ion at m/z 761 was produced by loss of 6‴-acetyl-5″-*O*-glucosyl-benzyl (CH_2-Ph-O-Glc-Ac, 310 Da) from parent ion $[M + Na]^+$. In ESI-MS^3 spectrum of compound **6** (Figure 3c), the ions at m/z 515 and 493 were generated by losing 2‴‴‴,6‴‴‴-diacetyl-glucosyl (Glc-2Ac, 246 Da) and 5‴‴-*O*-glucosyl benzyl (CH_2-Ph-O-Glc, 268 Da) from m/z 761, respectively. In ESI-MS^4 spectrum of compound **6** (Figure 3d), the fragment at m/z 247, 287, 269 were obviously observed. The ion at m/z 247 could be produced by ions at m/z 493 or 515, which suggested that the basic structure of compound 6 was 2-benzyl-malic acid. The ions at m/z 287 and 269 were obtained by loss of 2-benzyl-malic acid ($C_{11}H_{10}O_4$, 206 Da) and water molecule (H_2O, 18 Da) successively from m/z 493. Figure 4 showed the proposed fragmentation pathway of compound **6** **[20]**. The same rules were found in the MS^n analysis of other isolates listed in Table 3.

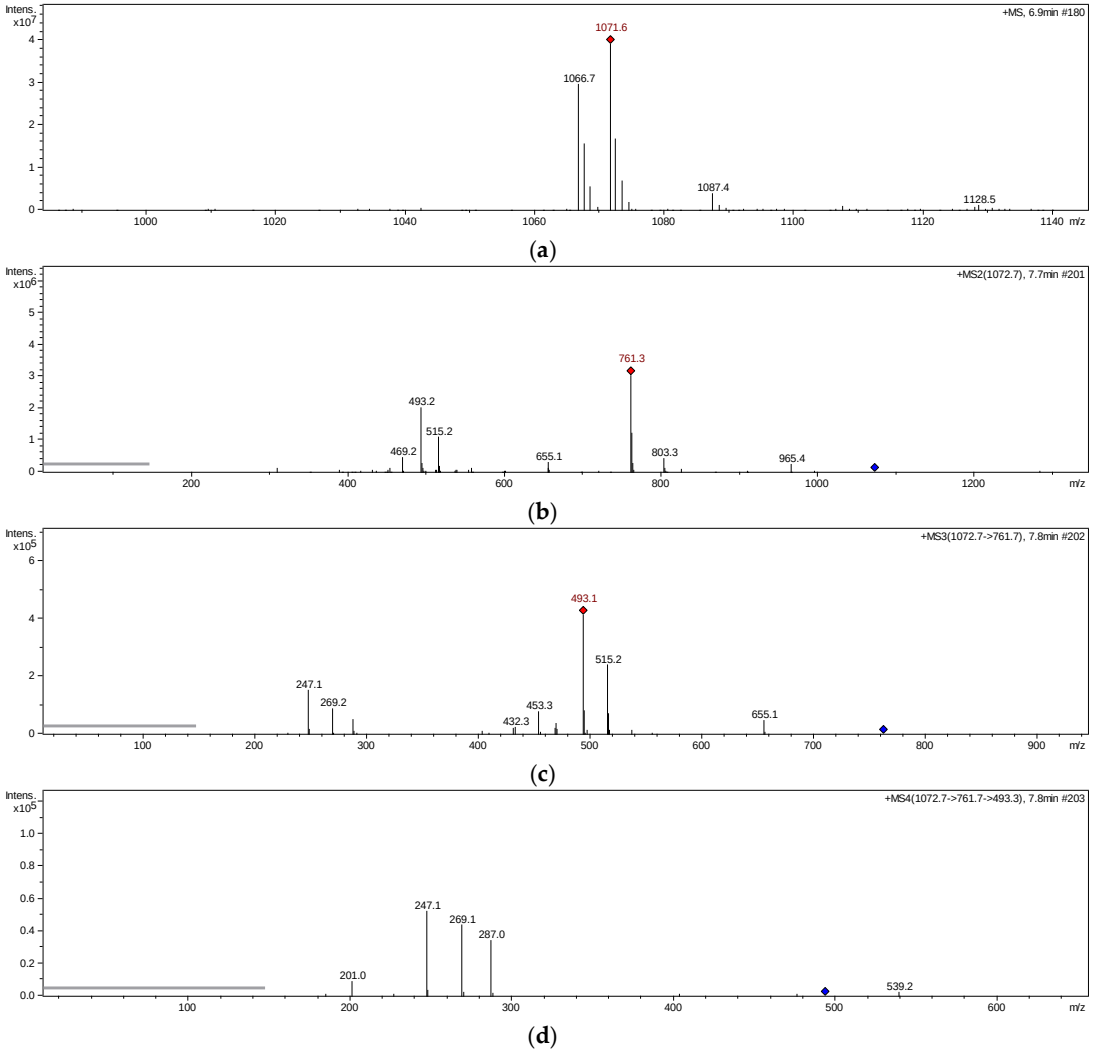

Figure 3. MS^n spectra of compound **6**. (**a**) Full-scan MS^1 spectrum, (**b**) ESI-MS^2 spectrum, (**c**) ESI-MS^3 spectrum, (**d**) ESI-MS^4 spectrum.

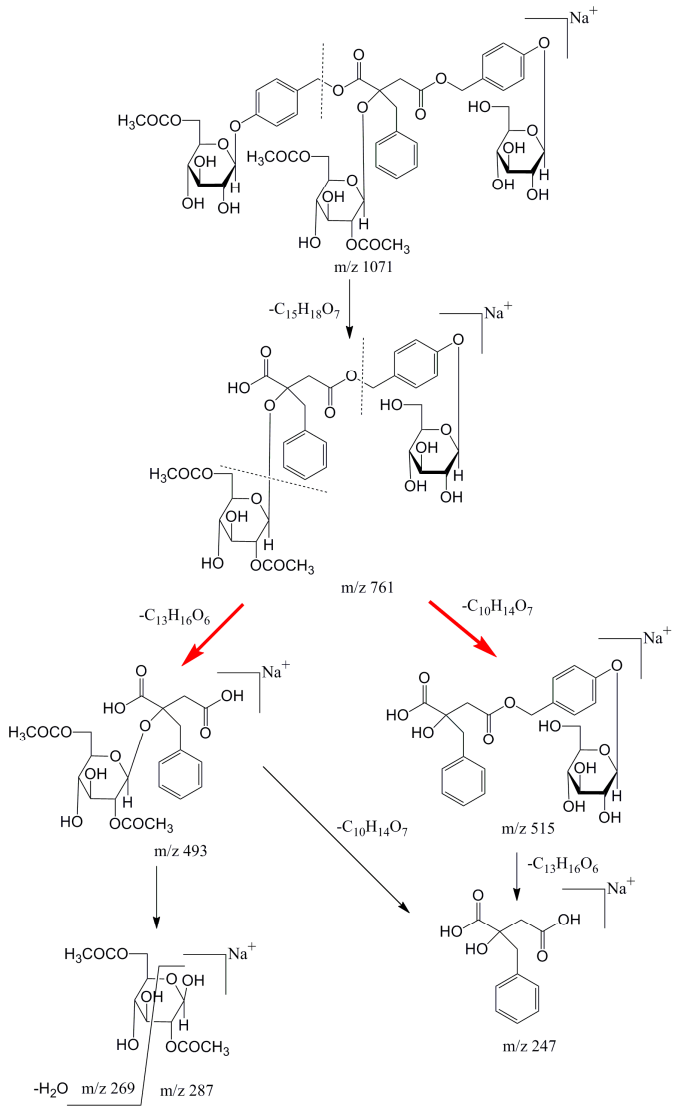

Figure 4. Proposed MS fragment pathway of compound **6**.

2.2.2. Structural Prediction of Glucosyloxybenzyl 2*R*-Benzylmalates Unreported

We also examined unknown glucosyloxybenzyl 2*R*-benzylmalate derivatives in fractions I~VI of *n*-BuOH extract with CH_3CN-H_2O (32:68, *v*/*v*) for mass spectrometry analysis. In the MS^n spectra, similar fragmentation pathways as described above were observed, and the possible structures of chemical components A1-A6, B1-B6, C1-C3, D1-D6 were inferred (Table 4). Herein, the analytic procedures were explained by peak A8 and A5.

The mass spectra of A8 contained significant ions at *m*/*z* 1108 $[M + NH_4]^+$, 1113 $[M + Na]^+$, 1129 $[M + K]^+$ (Figure 5a). Neutral loss of 268 Da (CH_2-Ph-O-Glc) and 310 Da (CH_2-Ph-O-Glc-Ac) were obtained from precursor ion at *m*/*z* 1113 to produce fragment ions at *m*/*z* 845 and *m*/*z* 535 in succession (Figure 5b,c). Then, the ion at *m*/*z* 329 obtained by loss of $C_{11}H_{10}O_4$ (206 Da) from *m*/*z* 535, combining the ion at *m*/*z* 247 (Figure 5d), indicated the presence of 2-benzyl-malic acid moiety in A8. Based on its fragmentation behaviors and previous studies, A8 was inferred to be the structure shown in Figure 6. Moreover, the mass spectra of A5 showed the same molecular formula and similar fragmentation ions with A8, but the retention time on HPLC with the same conditions were different, which indicated A5 was an isomer of A8. The succession of neutral loss of 310 Da and 268 Da obtained from the ion at *m*/*z* 845 produced by precursor ion at *m*/*z* 1113 suggested one of Ac groups in A5 was located at G2, and not at G1. The same experimental procedures were applied to analyze other molecules

list in Table 4, and the main fragments observed in MS^n spectra of the $[M + Na]^+$ precursor ions were summarized.

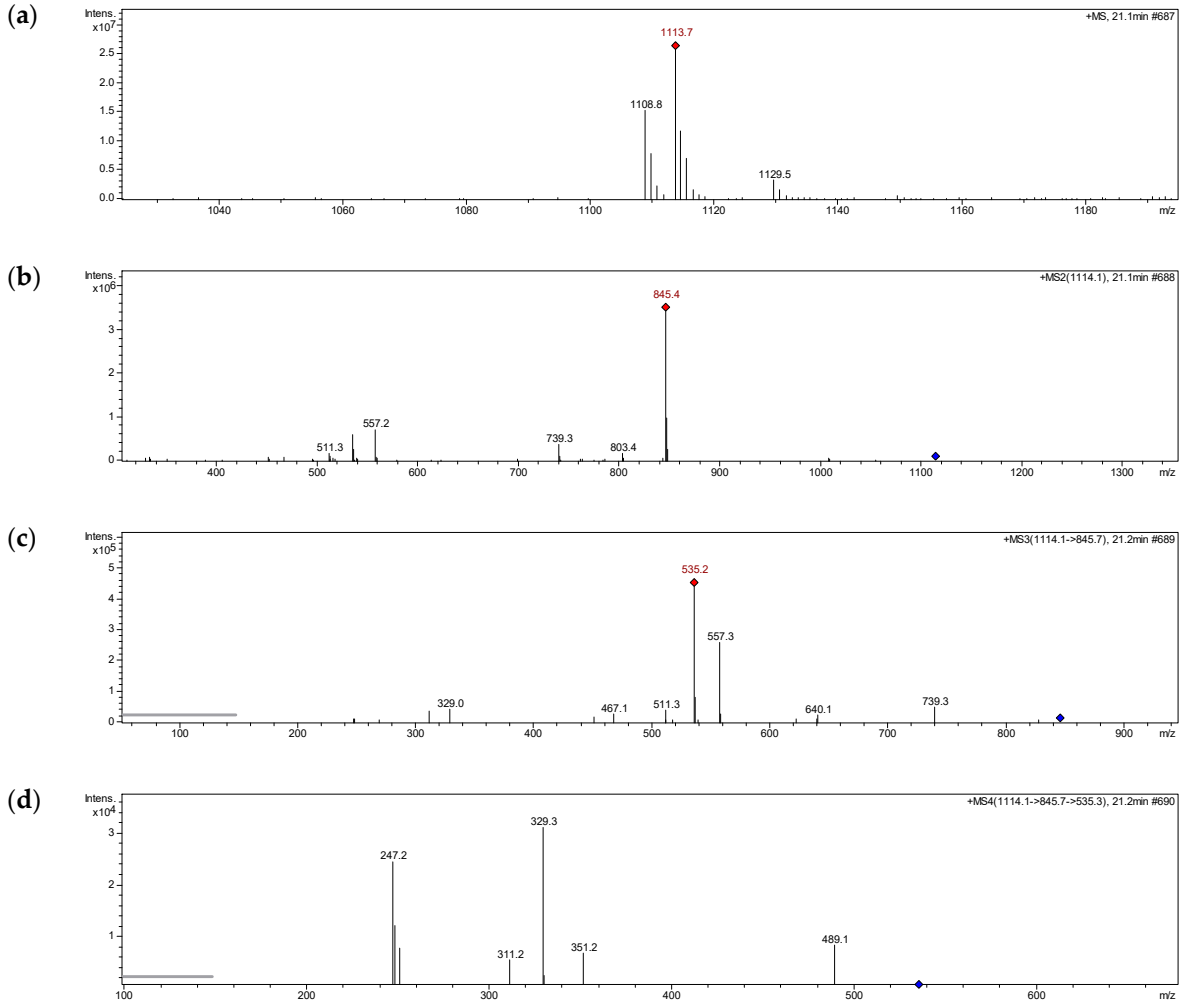

Figure 5. MS^n spectra of A8. (**a**) Full-scan MS^1 spectrum, (**b**) ESI-MS^2 spectrum, (**c**) ESI-MS^3 spectrum, (**d**) ESI-MS^4 spectrum.

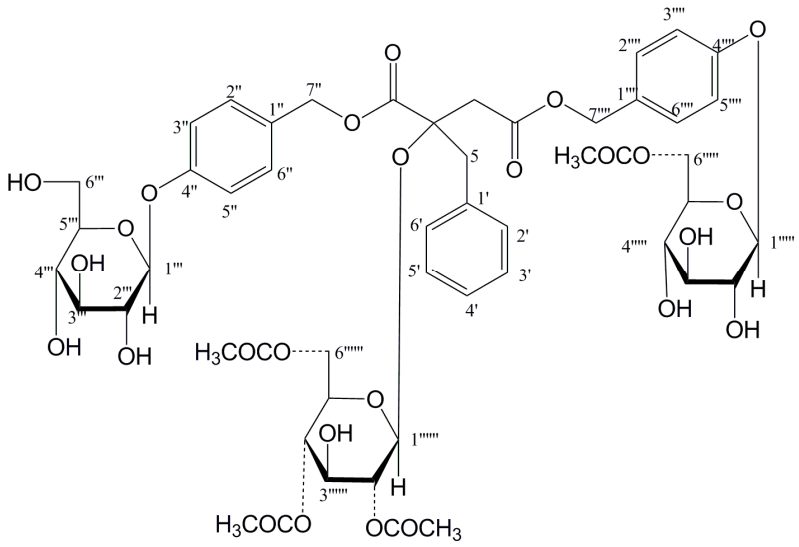

Figure 6. Proposed structure of A8.

2.3. Anti-hepatic Fibrosis Activity

Emerging studies indicated that HSC in resting state could be induced to activated state by LPS [21], while the inhibition of proliferation of activated HSC, has been considered as an effective target for liver fibrosis [22]. In addition, Considering the bioactive results obtained for the "BaoGan capsule" in our previous work, the anti-hepatic fibrosis activities of the isolates 1–8 were tested on the proliferation of LPS-activated HSC-T6 cells in vitro by MTS method. Legalon (silymarin capsules) was taken as a positive control. As shown in Figure 7, compound **1**, **2**, **4**, **5**, **8** were exhibited moderate anti-proliferative activity with significantly different values while the concentration was 100 μg/mL, while positive control showed a significant difference at 50 μg/mL.

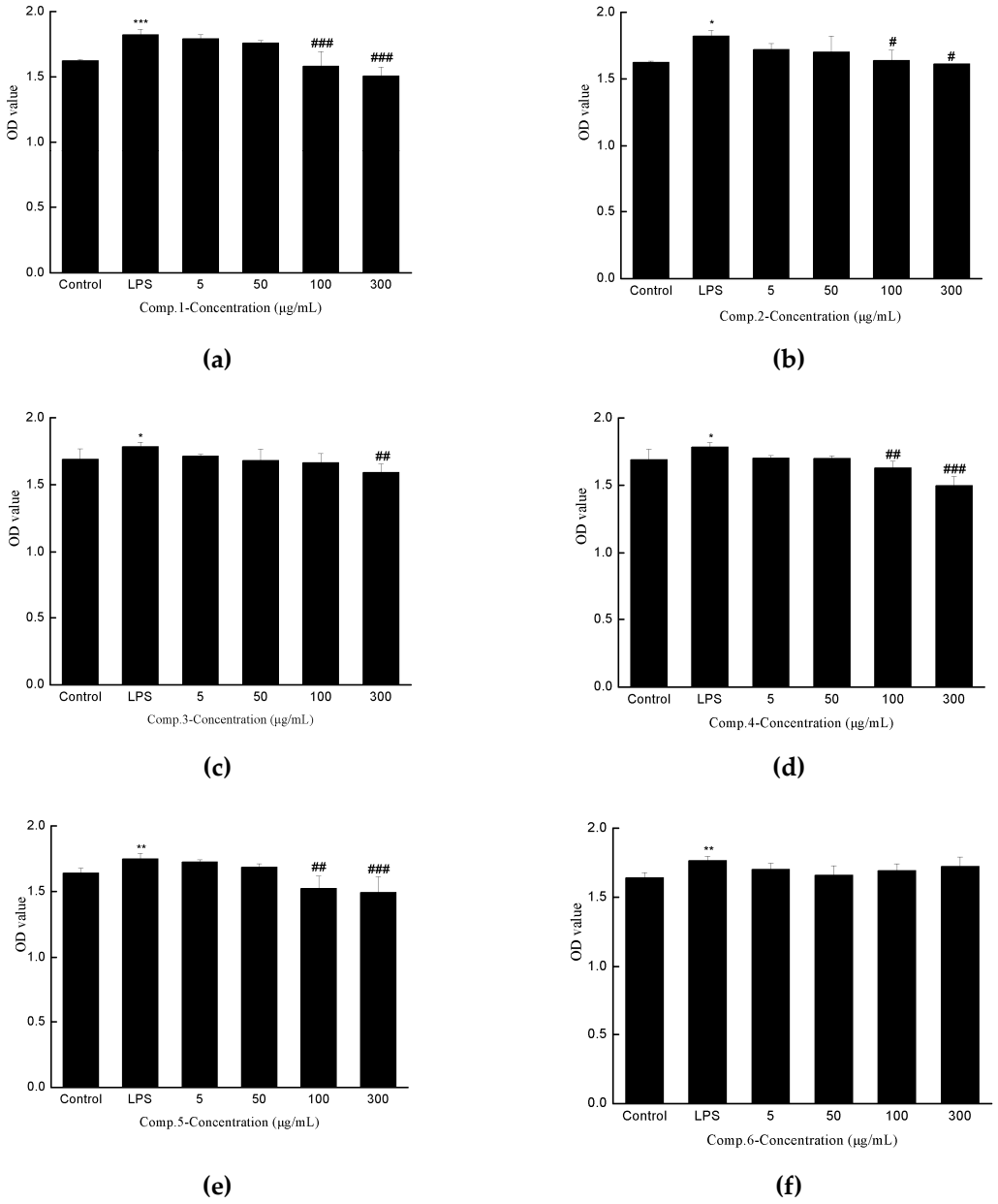

Figure 7. *Cont.*

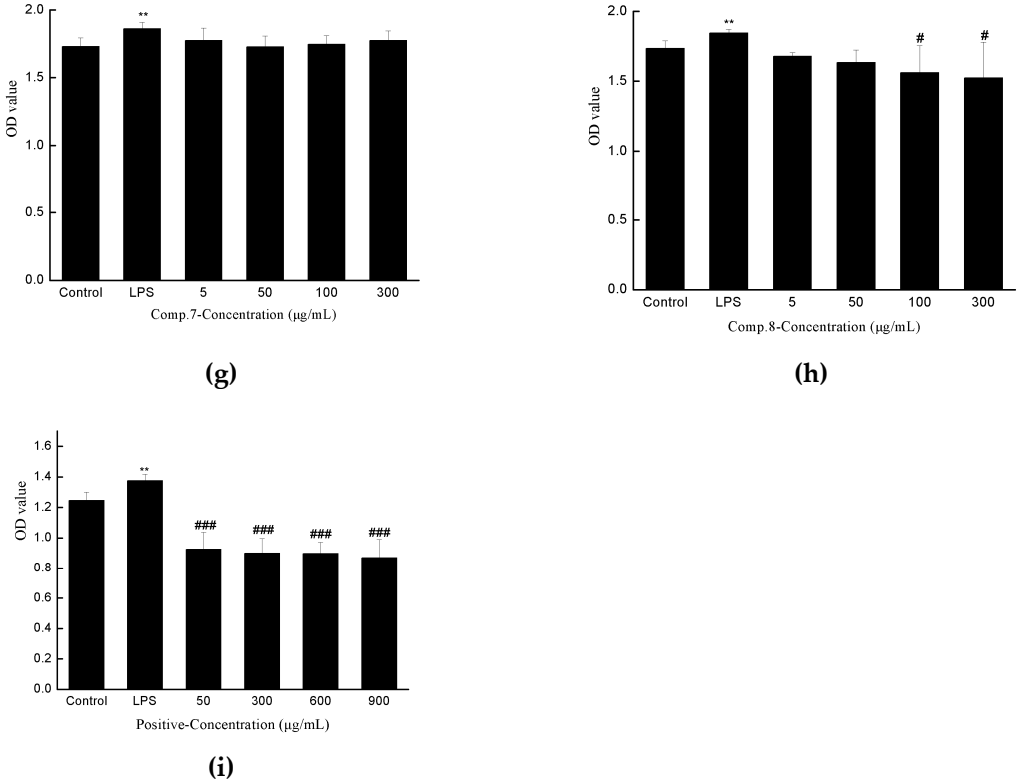

Figure 7. Inhibitory activity of compound **1** (**a**)–**8** (**h**) and positive control (**i**) on the proliferation of LPS-activated HSC-T6.

3. Materials and Methods

3.1. General Experimental Procedures

HPLC analyses were performed on Shimadzu LC-20AD (Shimadzu, Kyoto, Japan) equipped with a ZORBAX Eclipse XDB-C_{18} column (250 × 4.6 mm, 5 μm, Agilent, Santa Clara, CA, USA) and a SPD-20A detector. Preparative HPLC separations were conducted on a Shimadzu LC-6AD system with a preparative reversed-phase C_{18} column (250 × 20 mm, 5 μm, YMC-Pack ODS-A, Tokyo, Japan) and a SPD-6A detector. Mobile phase were purified water and methanol with chromatographic grade, which were bought from Merck. Organic reagents were analytical grade (Beijing Chemical Works, Beijing, China). One dimensional nuclear magnetic resonance (1D NMR: ^{1}H, ^{13}C, DEPT) and two dimensional nuclear magnetic resonance (2D NMR: HSQC, HMBC, ^{1}H-^{1}HCOSY) were measured on Bruker 700MHz AVANCE III spectrometer and Bruker AVANCE DRX-500 spectrometer (Karlsruhe, Germany) in DMSO-d_6 (Sigma-Aldrich, St. Louis, MO, USA). Chemical shifts are shown in δ (ppm) with tetramethylsilane (TMS) as an internal standard. High resolution-electrospray ionization-mass spectrometry (HR-ESI-MS) and High-performance liquid chromatography-electrospray ionization-multiple stage mass spectrometry (HPLC-ESI-MS^n) data were obtained from a 1100 Agilent Series coupled to an Agilent 6520 Accurate Mass Q-TOF and LC-MSD trap Mass spectrometer (Agilent Technologies, Santa Clara, CA, USA), respectively.

3.2. Plant Material

The whole plant of *A. graminifolia* was bought from Dai hospital of Xishuanbanna Autonomous Prefecture, Yunnan Province, China. A voucher specimen (batch number: 20111128) was collected in the laboratory.

3.3. Extraction and Isolation

Air dried powder of *A. graminifolia* (8.0 kg) was decocted with 80% ethanol (3 times, 2 h/time) at room temperature and extracting solution was merged and filtered. The filtrate was evaporated under reduced pressure to acquire crude extraction, which was further extracted with petroleum ether, chloroform, ethyl acetate and n-butanol to obtain the corresponding fractions. The *n*-BuOH extract was fractioned on a macroporous resin adsorption column eluting with ethanol/water (10:90, 50:50, 100:0, *v*/*v*) to yield 3 fractions (A–C). Fraction B (22.2 g) was subjected to Rp-18 silica gel column eluted with acetonitrile/water (10:90→100:0, *v*/*v*) to obtain five fractions (B1–B5). Fraction B3 **(**5.5 g**)** was then separated by silica gel column eluted with $CHCl_3$/CH_3OH (20:1, 2:1, 0:1) to give six fractions (I–VI). Fraction V (0.48 g) was submitted to preparative HPLC on a Rp-18 column (250 mm × 20 mm, wavelength 279 nm, flow rate 4 mL/min) with CH_3CN-H_2O (35:65, *v*/*v*) to give compound **1** (26.83 mg, RT = 21.5 min) and peaks D1~D6 eluted by CH_3CN-H_2O with 5 mM ammonium acetate (32:68, *v*/*v*). Fraction II (2.64 g) was eluted with CH_3CN-H_2O (29:71,*v*/*v*) to afford compound **2** (1.71 mg, RT = 5 min), compound **3** (1.62 mg, RT = 8.2 min) and compound **4** (3.84 mg, RT = 15.2 min), with CH_3CN-H_2O (26:74, *v*/*v*) to afford compound **5** (2.34 mg, RT = 25 min), compound **6** (3.18 mg, RT = 30 min) and compound **7** (1.85 mg, RT = 41.9 min), with CH_3CN-H_2O (30:70, *v*/*v*) to afford compound **8** (2.01 mg, RT = 42 min). Furthermore, a search of the rest of Fraction II was then conducted at 0.2 mL/min for HPLC-ESI-MS^n to obtain Peaks A1~A9 eluted by CH_3CN-H_2O with 5 mM ammonium acetate (30:70, *v*/*v*), peaks B1~B6 eluted by CH_3CN-H_2O with 5 mM ammonium acetate (26:74, *v*/*v*); peaks C1~C3 eluted by CH_3CN-H_2O with 5 mM ammonium acetate (27:73, *v*/*v*), and RT values of the peaks were shown in Table 4.

3.4. Cell Proliferation Inhibition Assay

3.4.1. Chemical and Reagents

LPS, RPMI-1640 medium, penicillin-streptomycin, and trypsin were bought from Solarbio, Beijing, China and fetal bovine serum were purchased from Sijiqing, Hangzhou, China. Dimethyl sulfoxide (DMSO), PMS and MTS [3-(4,5-dimethylthiazol-2-yl)-5-(3-carboxymethoxyphenyl)-2-(4-sulfophenyl)-2*H*-tetrazolium, inner salt] were purchased from Sigma-Aldrich (Steinheim, Germany).

3.4.2. In vitro Evaluation of Anti-Liver Fibrotic Activity

HSC-T6 cells were maintained in RPMI-1640 medium supplemented with 10% fetal bovine serum and 1% penicillin-streptomycin in an incubator with constant temperature at 37 °C and a humidified atmosphere of 5% CO_2. The cells were trypsinized and passaged to new plates every two or three days. HSC-T6 cells were seeded in 96-well plates (5×10^3/100 μL) for 24 h to ensure fully adhesion and good condition. The cell medium in the wells was changed into fresh RPMI-1640 medium supplemented with 5% fetal bovine serum for further incubation. Cells incubated with LPS (1 μg/mL) in the different concentration of compounds **1**~**8** (0, 5, 50, 100, 300 μg/mL) were cultivated for another 24 h. Each group was provided with 6 independent duplicates. Cell viability was determined using MTS/PMS assay. Absorbance values were read at 490 nm on an ELISA reader. 0.1% DMSO was considered as blank control and legalon (silymarin capsules) as positive control. Cell viability was expressed as a percentage of control cells at 100% viability. Statistical analysis was performed using origin Pro 8.0 (OriginLab Corpration, One Roundhouse Plaza, Northampton, MA, USA).

4. Conclusions

Glucosyloxybenzyl 2*R*-benzylmalates are a class of naturally occurring substances distributed in Orchidaceae. They were noticed for their novel type of structure and significant activities, while the research of glucosyloxybenzyl 2*R*-benzylmalates was limited by their higher polarity and less content. In present work, basis on the information acquired from HPLC-ESI-MS^n experiment combined with NMR analysis, it was possible not only to identify 8 compounds isolated from *A. graminifolia*, but also

to predict the structures of 24 previously unreported glucosyloxybenzyl 2*R*-benzylmalates in the extract. The ESI-MS^n experiments provide a useful guide for gaining the large structural information of novel compounds, which are important to drug design, although the analytical method cannot confirm the accurate substitution position of Ac groups of these glucosyloxybenzyl 2*R*-benzylmalates.

In addition, a cell model associated with hepatic fibrosis was established by using LPS to stimulate HSC-T6. The isolates were carried to hepatic fibrosis experiment while compounds **1**, **2**, **4**, **5**, **8** showed moderate anti-hepatic fibrosis effects. Nevertheless, the studies on the quantitative structure-antihepatic fibrosis relationship of predicted glucosyloxybenzyl 2*R*-benzylmalates will be further investigated.

5. Patents

Two patents resulting from the work about new structures, anti-liver fibrotic activity and MS fragment pathway have been submitted to the Chinese Patent Office.

Supplementary Materials: The following are available online: ^{1}H and ^{13}C NMR, DEPT135, HSQC, HMBC, ^{1}H-^{1}H COSY spectra of new compounds **2**, **5**, **6**, and **8**; HPLC-ESI-MS spectra of the isolates **1**–**8**; HPLC-ESI-MS^n spectra of peaks A1–A9, B1–B6, C1–C3, and D1–D6.

Author Contributions: Q.L. performed the isolation, MS analyses and structural identification of the compounds under the supervision of F.L. Original draft preparation was wrote by Q.L. and further reviewing and editing was completed by F.L. Q.L. and F.S. were in charge of the biological evaluation. In addition, F.L. provided significant advice regarding the NMR structural elucidation and MS deduction. Y.D. and R.D. contributed to the plant material selection and its resource. This paper was financially supported by F.L., Y.D., R.D.

Funding: This research was financially supported by National Natural Science Foundation of China (Grant No. 81503353) and the National Major Scientific Instruments and Equipment Development Project (Grant No. 2012YQ040140).

Conflicts of Interest: The authors declare no conflict of interest.

References

1. Jiang Su. New Medical College. *Dictionary of Chinese Traditional Medicine*; Shanghai Science and Technology Press: Shanghai, China, 1986; pp. 455–456.
2. Li, Y.K.; Zhou, B.; Ye, Y.Q.; Du, G.; Niu, D.Y.; Meng, C.Y.; Gao, X.M.; Hu, Q.F. Two new diphenylethylenes from Arundina graminifolia and their cytotoxicity. *Bull. Korean Chem. Soc.* **2013**, *34*, 3257–3260. [CrossRef]
3. Hu, Q.F.; Zhou, B.; Ye, Y.Q.; Jiang, Z.Y.; Huang, X.Z.; Li, Y.K.; Du, G.; Yang, G.Y.; Gao, X.M. Cytotoxic deoxybenzoins and diphenylethylenes from Arundina graminifolia. *J. Nat. Product.* **2013**, *76*, 1854–1859. [CrossRef] [PubMed]
4. Meng, C.Y.; Niu, D.Y.; Li, Y.K.; Zhou, B.; Ye, Y.Q.; Du, G.; Hu, Q.F.; Gao, X.M. A new cytotoxic stilbenoid from Arundina graminifolia. *Asian J. Chem.* **2014**, *26*, 2411–2413. [CrossRef]
5. Hu, Q.F.; Zhou, B.; Huang, J.M.; Gao, X.M.; Shu, L.D.; Yang, G.Y.; Che, C.T. Antiviral phenolic compounds from Arundina gramnifolia. *J. Nat. Prod.* **2013**, *76*, 292–296. [CrossRef] [PubMed]
6. Gao, Z.R.; Xu, S.T.; Wei, J.; Shi, H.L.; Hu, Q.F. Phenolic compounds from Arundina graminifolia and their anti-tobacco mosaic virus activities. *Asian J. Chem.* **2013**, *25*, 2747–2749. [CrossRef]
7. Li, L.; Xu, W.X.; Liu, C.B.; Zhang, C.M.; Zhao, W.; Shang, S.Z.; Deng, L.; Guo, Y.D. A new antiviral phenolic compound from Arundina gramnifolia. *Asian J. Chem.* **2015**, *27*, 3525–3526. [CrossRef]
8. Li, Y.K.; Yang, L.Y.; Shu, L.D.; Shen, Y.Q.; Hu, Q.F.; Xia, Z.Y. Flavonoid compounds from Arundina graminifolia. *Asian J. Chem.* **2013**, *25*, 4922–4924. [CrossRef]
9. Shu, L.D.; Shen, Y.Q.; Yang, L.Y.; Gao, X.M.; Hu, Q.F. Flavonoids derivatives from Arundina graminifolia and their cytotoxicity. *Asian J. Chem.* **2013**, *25*, 8358–8360. [CrossRef]
10. Niu, D.Y.; Han, J.M.; Kong, W.S.; Cui, Z.W.; Hu, Q.F.; Gao, X.M. Antiviral fluorenone derivatives from Arundina gramnifolia. *Asian J. Chem.* **2013**, *25*, 9514–9516. [CrossRef]
11. Zhu, H.; Song, Q.S. Chemical components of Arundina graminifolia. *Nat. Prod. Res. Dev.* **2008**, *20*, 5–7.

12. Meng, W.W.; Nan, G.; Lin, F.K.; Zhao, H.W.; Deng, Y.L.; Dai, R.J.; Chen, Y.; Huang, Y.M.; Zhao, Y.H. Effect of Baogan Yihao on Liver Fibrosis in Rats Induced by CCl4 and High-Fat Feeding. *Trans. Beijing Inst. Technol.* **2014**, *34*, 767–770.
13. He, P.P.; Song, C.C.; Meng, W.W.; Deng, Y.L.; Dai, R.J.; Lin, F.K.; Chen, Y.; Zhao, Y.H.; Huang, Y.M. Protective Effect of Baogan Yihao on Acute and Chronic Hepatic Injury. *Chin. J. Exp. Tradit. Med. Formul.* **2012**, *18*, 195–198.
14. Dai, R.J.; Su, J.; Wang, F.; Lin, F.K.; Lv, F.; Chen, Y.; Meng, W.W.; Deng, Y.L. The Protective Effects of BGYH on Mice Acute Liver Injury Induced by D-Galn and LPS. *Trans. Beijing Inst. Technol.* **2015**, *35* (Suppl. 1), 67–71.
15. Liu, X.J.; Su, J.; Shi, Y.; Guo, Y.; Suheryani, I.; Zhao, S.C.; Deng, Y.L.; Meng, W.W.; Chen, Y.; Sun, L.L.; Dai, R.J. Herbal Formula, Baogan Yihao (BGYH), Prevented Dimethyl-nitrosamine (DMN)-Induced Liver Injury in Rats. *Drug Dev. Res.* **2017**, *78*, 155–163. [CrossRef] [PubMed]
16. Auberon, F.; Olatunji, O.J.; Krisa, S.; Herbette, G.; Antheaume, C.; Bonte, F.; Merillon, J.M.; Lobstein, A. Arundinosides AG, new glucosyloxybenzyl 2R-benzylmalate derivatives from the aerial parts of *Arundina graminifolia*. *Fitoterapia* **2018**, *125*, 199–207. [CrossRef] [PubMed]
17. Morikawa, T.; Xie, H.; Matsuda, H.; Yoshikawa, M. Glucosyloxybenzyl 2-Isobutylmalates from the Tubers of Gymnadenia conopsea. *J. Nat. Prod.* **2006**, *69*, 881–886. [CrossRef] [PubMed]
18. Tatsis, C.E.; Boeren, S.; Exarchou, V.; Troganis, A.N.; Vervoort, J.; Gerothanassis, I.P. Identification of the major constituents of Hypericum perforatum by LC/SPE/NMR and/or LC/MS. *Phytochemistry* **2007**, *68*, 383–393. [CrossRef]
19. Song, J.; Dai, R.J.; Deng, Y.L.; Lv, F. Rapid structure prediction by HPLC-ESI-MS^n of twenty-five polyoxypregnane tetraglycosides from Dregea sinensis with NMR confirmation of eight structures. *Phytochemistry* **2018**, *147*, 147–157. [CrossRef]
20. Cai, M.; Zhou, Y.; Gesang, S.L.; Bianba, C.; Ding, L.S. Chemical fingerprint analysis of rhizomes of Gymnadenia conopsea by HPLC–DAD–MSn. *J. Chromatogr. B* **2006**, *844*, 301–307. [CrossRef]
21. Kao, Y.H.; Chen, P.H.; Wu, T.Y.; Lin, Y.C.; Tsai, M.S.; Lee, P.H.; Tai, T.S.; Chang, H.R.; Sun, C.K. Lipopolysaccharides induce Smad2 phosphorylation through PI3K/Akt and MAPK cascades in HSC-T6 hepatic stellate cells. *Life Sci.* **2017**, *184*, 37–46. [CrossRef]
22. Kang, K.B.; Jin, B.J.; Kim, J.W.; Kim, H.W.; Sung, S.H. Ceanothane- and lupane-type triterpene esters from the roots of Hovenia dulcis, and their antiproliferative activity on HSC-T6 cells. *Phytochemistry* **2017**, *142*, 60. [CrossRef] [PubMed]

Sample Availability: Samples of the compounds are not available from the authors.